Diffuse elastic scattering of atoms from surface steps

C. W. Skorupka* and J. R. Manson
Department of Physics and Astronomy, Clemson University, Clemson, South Carolina 29634-1911
(Received 13 October 1989)

We investigate the diffuse elastic scattering of thermal-energy helium atoms from step defects on close-packed metal surfaces. A semiclassical approximation is developed and applied to hard-wall step profiles to model the broad oscillations observed in experiments. The observed fine structure is investigated with lattice-gas models together with a minimum distance between steps caused by the repulsive step-step interaction. The effects of an attractive adsorption well and kink defects along the steps are considered. The fine structure appears to be well explained by a lattice-gas model.

I. INTRODUCTION

The surface properties of solids can be quite different from those of the bulk. The topmost layers of a solid can exhibit reconstruction and relaxation phenomena, surface vibrational modes, and a variety of phase transitions. These surface properties can be sensitive to the presence of defects such as steps, kinks, and adsorbed species. It is important, therefore, to be able to characterize the type, distribution, and behavior of surface defects. Rare-gas-atom scattering provides a useful tool for such characterization.[1]

Much information has been obtained on the distribution and dynamics of defects and adsorbates through observations of their total cross sections on the surface.[2] The total cross section is readily determined through measurements of the decrease in intensity of the diffraction peaks as a function of coverage.[3] Recently, it has been demonstrated that the differential cross section of a defect or adsorbate on a surface can be measured by observing the diffuse elastic background.[4,5] Specific experiments involve the observation of single steps on a clean Pt(111) surface,[4] and very low coverages of adsorbed CO on flat Pt(111).[5] The cross section is usually measured as a function of scattering angle or of parallel momentum transfer, and the characteristic signature is a series of broad oscillations in intensity. The origin of these oscillations is attributed to interference between scattering from different sections of the hard-core profile, and to interference with multiple scattering between defect and the flat surface. These oscillations give directly the dimension of the hard-core profile of the step or adsorbate, and more detailed comparison with models can give specific information on the shape of the profile.[6,7]

In this paper we use a Green-function formalism of scattering theory to develop a semiclassical approximation for the diffuse intensity scattered from the hard-core profile of an adsorbate or defect. This is applied to several hard-wall step profiles in order to model the broad oscillations observed in the diffuse He scattering experiments. The possibility of an attractive well in the vicinity of a step edge is incorporated in the model with a simple refraction transformation. Best-fit models for the available data are obtained and compared with earlier work.[6,7]

The experiments on diffuse elastic scattering by steps on the Pt(111) surface exhibited, in addition to the broad oscillations, several instances of fine structure in the intensity which usually appeared in the vicinity of a diffraction peak position. We attribute this fine structure to diffraction from the step defects distributed on lattice sites. We consider a number of lattice-gas models which include the roles of multiple terrace levels, the *ABC* stacking symmetry of the fcc (111) surface, and the minimum cutoff distance between adjacent steps due to their mutual repulsive interaction. Good agreement with the scattering data is obtained.

II. SCATTERING MODEL

The initial experiments on the large-angle diffuse elastic scattering from low densities of surface defects interpreted the observations as due to reflections from isolated defects.[4,5] The broad intensity oscillations are caused by interference between the amplitude directly scattered from the defect and the amplitude doubly scattered with a backreflection from the surface; or depending on the surface profile of the defect, there can be strong interference between amplitudes scattered from two separated regions of the profile (this latter possibility is the semiclassical supernumerary rainbow). In either case, as compared to the problem of scattering from isolated defects in a vacuum, the major role of the flat surface is to give a mirror reflection to the amplitude that would have been forward scattered and cause it to interfere with the amplitude backscattered from the defects. This situation can be viewed as the amplitude scattered from an isolated defect interfering with a phase-shifted amplitude coming from an image of the defect beneath the surface which is illuminated by a beam incident symmetrically from below. Because of the analogy of this situation with the symmetry oscillations observed in the scattering of identical elementary particles, the observed intensity pattern has been called "reflection-symmetry oscillations."[4]

The theory of diffuse elastic and inelastic scattering by isolated surface defects has been examined recently, and in the case of a dilute distribution with no multiple scattering between defects the scattered intensity can be expressed in the standard manner of a form factor multiplying a structure factor which depends only on the distribution of defects.[8] Briefly, the scattered intensity is proportional to the transition rate $w(\mathbf{k}_f,\mathbf{k}_i)$ for the scattering from initial state $\mathbf{k}_i$ to final state $\mathbf{k}_f$:

$$w(\mathbf{k}_f,\mathbf{k}_i)=\frac{2\pi}{h}\langle |T_{fi}|^2\,\delta(E_f-E_i)\rangle \ , \tag{1}$$

where T_{fi} is the transition matrix, E_f and E_i are the initial and final total energies, and the angular brackets signify an average over crystal vibrations as well as the average over defect distributions. The Van Hove transformation[9] can be used to write this in terms of the Fourier transform of a time-ordered correlation function

$$w(\mathbf{k}_f,\mathbf{k}_i)=\frac{1}{\hbar^2}\int_{-\infty}^{\infty} dt\, e^{-i(\varepsilon_f-\varepsilon_i)t/\hbar}\langle T_{\rm if}(0)T_{fi}(t)\rangle \ , \tag{2}$$

where $\varepsilon_{f,i}$ are particle energies and the time dependence of the T operator is dictated by the crystal Hamiltonian H_c in the interacting picture according to

$$T(t)=e^{iH^c t/\hbar}Te^{-iH^c t/\hbar} \ . \tag{3}$$

The assumption of identical, nondeformable, independent scatterers allows one to separate out the time dependence of the transition matrix as

$$T_{fi}(t)=\tau(\mathbf{k}_f,\mathbf{k}_i)\sum_j e^{i\mathbf{k}\cdot\mathbf{r}_j(t)} \ , \tag{4}$$

where $\mathbf{r}_j(t)$ is the position of the jth defect. We are interested in elastic scattering from stationary defects so that $\mathbf{r}_j$ is independent of time. Then Eq. (4) becomes

$$w(\mathbf{k}_f,\mathbf{k}_i)=\frac{2\pi}{h}|\tau(\mathbf{k}_f,\mathbf{k}_i)|^2\left\langle\sum_{j,n} e^{i\mathbf{k}\cdot(\mathbf{r}_j-\mathbf{r}_n)}\right\rangle\delta(\varepsilon_f-\varepsilon_i) \ . \tag{5}$$

Equation (5) shows the decomposition of the transition rate into the product of the form factor $F=|\tau(\mathbf{k}_f,\mathbf{k}_i)|^2$ and structure factor $S(\mathbf{k})$ with $\mathbf{k}=\mathbf{k}_f-\mathbf{k}_i$ given by

$$S(\mathbf{k})=\left\langle\sum_{j,n} e^{i\mathbf{k}\cdot(\mathbf{r}_j-\mathbf{r}_n)}\right\rangle \ , \tag{6}$$

where the angular brackets now signify an average over defect positions.

The remainder of this paper is concerned with the calculation of both the form factor and structure factor for helium atoms scattered by step defects on an otherwise flat surface substrate. It is important to recognize that the diffuse scattering can be divided into two distinct regimes: the region of small parallel momentum transfer scattered at small angles from the specular direction, and that of large angles or large momentum transfer. The small-angle scatering intensity is very large and is dominated by the contributions from the soft, long-ranged Van der Waals part of the interaction potential. The large-range scattering, of interest here, is several orders of magnitude smaller in intensity and is primarily due to interactions with the hard-core part of the interaction potential. Consequently, for calculating the form factor for the large-angle diffuse scattering we will use a hard repulsive wall potential with the possibility of an attractive well in front. In the next section we develop a Green-function method for calculating the form factor, and Sec. IV presents the results of model calculations together with the comparison with experiment and other recent theories. In Sec. V we take up the question of the structure factor.

III. THE FORM FACTOR

The first approach to calculating the form factor for the diffuse scattering of helium from a distribution of steps on a Pt(111) surface adopted a very simple model,[4] that of a half cylinder on top of a flat mirror. In spite of the lack of sophistication of this model, a reasonable fit to the data was achieved and a good estimate of the size of the hard-core potential of the step was obtained.

Drolshagen and Vollmer used the semiclassical wave-packet method, with an exponentially repulsive "soft-wall" potential and no attractive well. The step profile used was somewhat more realistic, the two terraces on either side of the step were joined by a smoothly varying fifth-order polynomial. A reasonable fit to the experimental data was obtained and the size of the hard-core estimated in Ref. 4 was verified.[6,10]

An even better agreement with experiment for the reflection symmetry oscillations has been obtained by Hinch[7,11] using a hard-wall profile in the eikonal approximation of Garibaldi *et al.*[12] The profile used by Hinch is a simple inclined plane, rounded off at each end with segments of circles. With it one can vary independently the width of the step, the height, and the slope of the incline. More recently, using a modified version of the sudden approximation, Hinch has investigated the role of the attractive adsorption well in front of the step.[13] The best fit with experiment was with a well having a depth that varied across the face of the step.

In this paper we wish to consider a different approach to the problem of calculating the form factor based on Green-function methods for a hard-wall profile. The step is treated as an isolated defect and the scattering amplitude is first calculated as if it were an atomic scattering problem with a highly nonsymmetric scattering center. The effect of the surface is then taken into account by adding to the direct scattering amplitude the amplitude from the image beneath the surface, with the correct phase difference of π.[4,14] The use of images is not strictly correct because the surface in the presence of an isolated step is not flat, but has two different terrace levels. However, because of the configuration of the experiment (mainly because of the fixed angle maintained between incident beam and detector) the overwhelming majority of the backreflected amplitude is reflected by only one of the terraces, and the contribution of the other terrace can be neglected. This point was carefully checked and found to

be true for all incident angles and energies used in the experiment.

Scattering from a hard wall involves solving the free-particle Schrödinger equation with the boundary condition that the wave function vanishes of the surface S. We write the wave function as $\psi=\psi_0+\psi_S$ with ψ_0 the incoming wave and ψ_S the outgoing scattered wave. Then the Green-function solution can be written as[15]

$$\psi=\psi_0+\frac{1}{4\pi}\int ds\,\hat{\mathbf{n}}\cdot[\psi_0\nabla G(\mathbf{r}|\mathbf{r}')-G(\mathbf{r}|\mathbf{r}')\nabla\psi_s]\ , \tag{7}$$

where G is the Green function and $\hat{\mathbf{n}}$ is the unit vector outward normal to the surface. In the semiclassical limit, where the wavelength is smaller than the smallest characteristic feature on the surface, it is a good approximation to break up the surface into illuminated and shadow regions. The illuminated hard-wall surface acts like a locally flat mirror, so the normal gradients of the reflected and incoming waves are equal:

$$\hat{\mathbf{n}}\cdot\nabla\psi_s=\hat{\mathbf{n}}\cdot\nabla\psi_0\ . \tag{8}$$

In the shadow region, both the wave function and its normal gradient vanish on the surface S:

$$\begin{aligned}&\hat{\mathbf{n}}\cdot\nabla\psi_s|_S=-\hat{\mathbf{n}}\cdot\nabla\psi_0|_S\ ,\\ &\psi_s|_S=-\psi_0|_S\ .\end{aligned} \tag{9}$$

The shadow, or Fraunhofer, part is strongly projected in the forward direction and is dependent on the end points or border line of the shadow region, and otherwise independent of the shape of the object in the region. The presence of the surface reflects the forward amplitude in the specular direction, so the shadow contribution is strongly peaked about the specular direction. The illuminated face contribution dominates the large-angle scattering. Combining Eqs. (8) and (9), the scattered wave function is

$$\begin{aligned}\psi_s=&-\frac{1}{4\pi}\int_{\substack{\text{illuminated}\\ \text{face}}} ds\,\hat{\mathbf{n}}\cdot[\psi_0\nabla_n G+G\nabla_n\psi_0]\\ &-\frac{1}{4\pi}\int_{\text{shadow}} ds\,\hat{\mathbf{n}}\cdot[\psi_0\nabla_n G-G\nabla_n\psi_0]\ .\end{aligned} \tag{10}$$

After choosing a profile we carry out the surface integral numerically, using the Green function for two- or three-dimensional geometry, whichever is appropriate. We note that Eq. (10) is a type of eikonal or Kirchhoff approximation, but it has an advantage over the method of Garibaldi *et al.*[12] in that it is good for all scattering angles, rather than being restricted to near specular scattering. This is an important characteristic for calculating the large-angle scattering from defects.

For most profiles Eq. (10) can also be integrated analytically using the stationary phase approximation. This is often called the primitive semiclassical approximation.[16] A major disadvantage of the stationary phase approximation is that it fails at an inflection point of the profile, and an infection point is very important because it dictates the rainbow scattering. Furthermore, the stationary phase approximation is valid only in the extreme semiclassical limit of very short wavelengths. The numerical integration eliminates all problems associated with inflection points, and appears to considerably extend the range of validity to larger wavelengths. We have checked the case of the profile of a half cylinder on a flat surface where the stationary phase solution is particularly simple. The two methods of solution agree only when $a/\lambda>20$, where a is the radius of the cylinder.

IV. FORM-FACTOR CALCULATIONS

Before calculating the form factor it is necessary to choose a hard-wall profile for the step. In order to facilitate this study we set a number of criteria to be obeyed by the profile; it should be smoothly and monotonically varying between the two terrace levels, the slope should vanish at the endpoints to match that of the terraces, and the height, width, and maximum slope should be independently variable parameters within reasonable limits. A step profile which meets all these criteria is

$$\phi(x)=\begin{cases}(h/2)[1-(2x/w)^r], & 0<x<w/2\\ (h/2)(2-2x/w)^r-h/2, & w/2<x<w\end{cases} \tag{11a}$$

(11b)

with

$$r=(w/h)\tan(\theta_m)\ . \tag{11c}$$

We take a notation in which z is the normal direction away from the surface and x is the axis parallel to the surface and perpendicular to the steps. Then in Eq. (11), h is the height difference between terraces, w is the width of the step, and θ_m is the maximum slope.

A number of calculations were carried out in a parameter fitting process in order to find the profile which best fits the experimental data. Choices of parameters in the ranges of $\theta_m=30°-37°$, $w=6.4-6.8$ Å, and with h the bulk value of 2.27 Å for Pt(111), all give an equally good fit. However, the fit was not particularly satisfactory. The large oscillations appear in the same positions as in the experimental data, but the amplitude of the oscillations at smaller values of parallel momentum transfer ΔK are too small, while some peaks at larger ΔK are too large and broad. Similar problems were noted in previous calculations.[6,7] There is reason not to place undue faith in the best-fit profile abstracted from simple hard-wall models. There models neglect the presence of an attractive well associated with the surface and there is evidence that this well is distorted by the step face.[13] The well depth of clean Pt(111) has been estimated at between 5 and 12 meV.[17] We chose to model the well by a simple refraction of the incoming and outgoing beam.[18] That is to say, the energy of the particle in the well is increased by the well depth D, while momentum is conserved parallel to the well edge. The well edge above the terraces is parallel to the surface, while over the step profile it is taken to be a straight line tilted at an angle θ_w which is roughly parallel to the maximum slope of the step. This refraction correction applies only to the illuminated face contributions. The shadow or Fraunhofer terms are not refracted by the well since they do not depend on the par-

ticulars of the shape of the illuminated face, but arise from the removal of intensity from the specular beam. The treatment of the shadow term is not critical in these calculations, since its contribution appears predominantly in the specular direction and the specular regime is dominated by scattering from the terraces in actual experiments.

Best fits of this model are compared to experiment in Figs. 1 and 2. For both graphs the values of the parameters are $\theta_m = 36°$, $w = 6.6$ Å, $h = 2.27$ Å, $\theta_w = 35°$, and a well depth of 9 meV. Figure 1 is for an incident wave vector of 7.9 Å and Fig. 2 for 9.7 Å. In both figures the positions and widths of the broad oscillations are in good agreement with experiment. We note that the profile inflection angle θ_m is in agreement with the observations of Lapujoulade *et al.* for the diffraction of He from ordered stepped surfaces of Cu, where the same angle corresponded to the rainbow position in the diffraction peak intensities.[19] There is considerable fine structure in the data that is not, and cannot, be explained by scattering from a single smooth profile model such as that used here. This fine structure is due to collective effects of the distribution of steps and we consider this in the next section where we look at the structure factor. We should also note that there are additional effects that can occur in the form factor that are outside of the scope of a hard-core model. A soft repulsive potential together with a long-range attractive well can give rise to additional rainbow and glory features, and a discussion of some of these possibilities is given by Yinnon *et al.*[20]

V. THE STRUCTURE FACTOR

The stepped Pt(111) data exhibit fine structure at and about reciprocal lattice vector positions occurring at values of ΔK equal to multiples of 2.7 Å^{-1}. The fine structure appears as split peaks, which occur only in the vicinity of maxima in the broad oscillations. This contrasts with the clean Pt(111) surface data, which are smooth and monotonically decreasing except for very

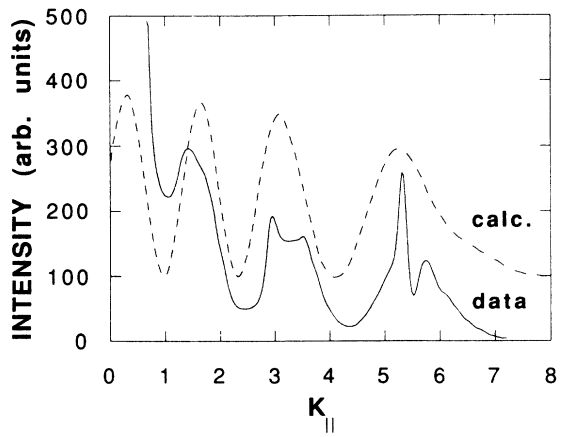

FIG. 1. The calculated form factor compared with experimental data for an incident wave vector of 7.9 Å^{-1}. The upper curve is the calculation and the lower curve is the data.

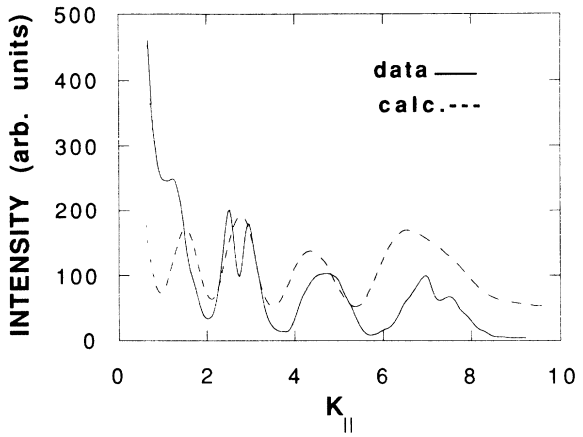

FIG. 2. Same as Fig. 1 except for an incident wave vector of 9.7 Å^{-1}.

weak diffraction peaks. Hinch[7] has suggested that the fine structure is due to scattering from a proposed Friedel-oscillation-like enhanced corrugation of the terraces in the vicinity of a step edge. This is likely only a partial explanation, however, since the fine structure can be seen at large ΔK, and only an extremely large corrugation could give a significant amount of intensity beyond the first-order diffraction peak. We are suggesting here that the source of the fine structure is not due to details in the form factor of a single step. Instead, it is due to correlations between scattered amplitudes from different steps.

Since the fine structure is associated with the broad oscillations due to scattering from the step edge, since it occurs at large ΔK, and both broad and fine structure can be wiped out by adsorption of CO (which selectively adsorbs at step sites),[4] it can be concluded that the fine structure arises from the interference between steps distributed on lattice sites in some random fashion. To model the fine structure we will use a lattice-gas distribution with a fixed minimum nearest-neighbor distance. This cutoff distance introduces a new length scale L on the surface in addition to the lattice spacing a. As the lattice parameter gives rise to diffraction peaks at $\Delta K = 2\pi/a$, the longer distance L introduces smaller ΔK oscillations in the intensity of approximate spacing $2\pi/L$.

We have shown in Eq. (5) that the scattering from a collection of isolated defects on a surface can be written as a product of an atomic form factor and a dynamical structure factor. The structure factor, which is shown in Eq. (6), contains all information about the relative positions of the defects whose number is N_D. For a completely random distribution, $S(\mathbf{k})$ is a constant equal to the number of defects. For a perfect lattice, it is a sum of δ functions over all reciprocal-lattice vectors $\mathbf{G}$:

$$S(\mathbf{k}) = N_D^2 \sum_{\mathbf{G}} \delta(\mathbf{k}-\mathbf{G}) \, . \tag{12}$$

For a finite lattice of N scattering centers with no vacancies, these δ functions are broadened by some width proportional to $1/N$. For a partially (randomly) filled lattice

with N_S lattice sites, $S(\mathbf{k})$ will have diffraction peaks broadened by $1/N_s$ and a constant background proportional to N_D.[19]

In a real scattering experiment there is a finite amount of angular and energetic spread in the incident and scattered beams, as well as a finite width in the detector opening.[21–23] The main effect of these instrumental limitations is to further broaden features in the scattered intensity over both energy and angles. However, the complete theoretical description of this broadening has been the object of considerable discussion over a number of years. In order to introduce these experimental broadening effects into a theory calculated for an ideal system, it is usually adequate to convolute the calculated intensity with an appropriate sharply peaked function.[7,24,25] Examples of such functions are the Lorenzian[7] or the Gaussian.[24,25] Explicitly, we simulate the experimental broadening effects as

$$I_{\text{meas}}(\mathbf{k})=I_{\text{ideal}}(\mathbf{k})\circ T_{\text{instr}}(\mathbf{k}) . \tag{13}$$

Following the approach of Houston and Park,[24] the pair correlation-function formalism is adopted. Briefly, the structure factor $S(\mathbf{k})$ is the Fourier transform of the pair correlation function $S(\mathbf{r})$, where

$$S(\mathbf{k})=\int d\mathbf{r}\, e^{i\mathbf{k}\cdot\mathbf{r}}S(\mathbf{r}) . \tag{14}$$

$S(\mathbf{r})$ is then calculated from the sum

$$S(\mathbf{r})=\sum_{\mathbf{r}'} P(\mathbf{r})P(\mathbf{r}-\mathbf{r}')\delta(\mathbf{r}) , \tag{15}$$

where $\mathbf{r}'$ goes over all lattice positions, and $P(\mathbf{r})$ is the density function which is 1 or 0 for filled or empty lattice sites, respectively. The convolution with the instrument function can be done in real space, where the effect is to multiply $S(\mathbf{r})$ by the Fourier transform of $T(\mathbf{k})$:

$$S_{\text{meas}}(\mathbf{k})=\int d\mathbf{r}\, e^{i\mathbf{k}\cdot\mathbf{r}}S(\mathbf{r})T(\mathbf{r}) . \tag{16}$$

Two different methods were employed to calculate the structure factors for the models studied here. In the first method, one begins by specifying the defect positions $\mathbf{r}_j$ according to a set of rules determined by the distribution. For example, in the random lattice-gas distribution, the probability of a site being occupied by a defect is equal to the density (ratio of number of defects to number of sites). A random number generator is then used to test each site for occupancy. These defect positions are then used to calculate the sum in (6). This ideal structure factor is then convoluted with a sharp instrument function, in this work the Gaussian form

$$T(\mathbf{k})=e^{-(\Delta K)^2/2b^2} . \tag{17}$$

A width $b=0.02$ Å^{-1} is used throughout this work. This particular value was chosen to be close to the width of the actual instrument used to obtain the Pt(111) data presented here. The convolution integral

$$S_{\text{meas}}(\mathbf{k})=\int d\mathbf{k}'\, S(\mathbf{k}')T(\mathbf{k}-\mathbf{k}') \tag{18}$$

is then calculated numerically. Although the method is very straightforward to implement, it has the disadvantage that for distributions with low densities of defects a large amount of computer time is required. This is because, as the density of defects decreases, a larger size lattice has to be sampled. The sum in (6) becomes a more rapidly oscillating function in ΔK, and in order to properly evaluate the convolution integral (18), one must evaluate or sample (6) at a rate greater than the fastest ΔK oscillation.

A second method which is based on the pair correlation formalism described above exploits the fact that the instrument function acts as a low-pass filter, which diminishes the contributions of the higher frequency and smaller ΔK oscillations. One begins by inserting (15) into (16) which converts the integral into the sum (written here in one-dimensional form for simplicity)

$$S(\Delta K)=\sum_m e^{i\Delta K x}S(x=ma)T(x=ma) . \tag{19}$$

One need only evaluate $S(x=ma)$ up to the transfer width of the instrument function, which for our choice of $b=0.02$ Å^{-1} corresponds to about 300 Å. The lattice spacing of Pt(111) is $a=2.32$ Å, so the largest m term is of the order of 100. Even though the lattice positions must still be evaluated for a large lattice, there is a substantial savings in computer time. This savings made it practical to utilize this method for extensive parameter searches for a large number of model distributions.[26,27]

We begin by considering a one-dimensional distribution of steps, that is to say a system in which all of the steps lie in the same plane. This sort of distribution is appropriate for the case of a perfectly flat surface with two terrace levels connected by alternating up and down steps. We model the repulsive interaction between steps by assuming a minimum cutoff length or minimum nearest-neighbor distance between defects. This one-dimensional distribution is generated by specifying the probability function $P(m)$, which is the probability of finding the next defect at lattice position $i+m$, given a defect at position i. This type of distribution belongs to the class known as Markov chains.[28] For the random lattice gas with a minimum cutoff distance L, $P(m)$ is zero for all m up to L, and then the probability is the geometric distribution given by γ, $\gamma(1-\gamma),\ldots,\gamma(1-\gamma)^{m-L}$, where γ is related to the density of defects ρ by $\gamma=\rho/(1-L\rho)$.

Figure 3 shows the structure factor for this distribution. The cutoff parameter is varied while the density is held constant at a value of $\rho=0.1$. The cutoff length gives rise to the "side bands" or satellite peaks which appear around the diffraction peak positions occurring at multiples of $\Delta K=2.7$ Å^{-1}. This work is consistent with the work of Lent and Cohen,[28] who studied the diffraction from terraces with various step distributions. We have also studied a number of models with a "soft" cutoff, in which instead of $P(m)=0$ for all $m<L$, $P(m)$ is allowed to increase from zero at $m=0$ to join the geometric distribution at $m=L$. The effect of all reasonable soft cutoffs was to wash out the satellite oscillations away from the diffraction peaks, but the satellites nearest to the diffraction peaks change very little.

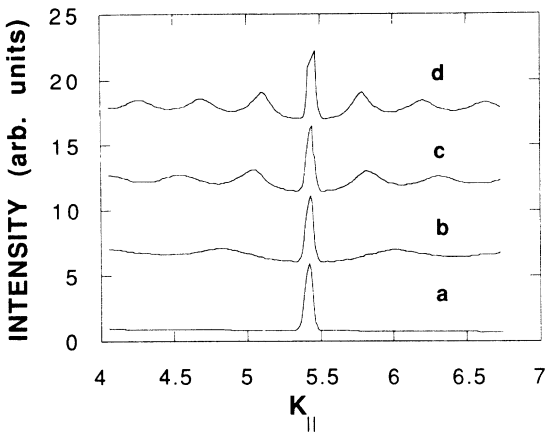

FIG. 3. The structure factor for different reduced cutoff lengths L for the one-dimensional distribution. The reduced density ρ is 0.1. a, $L=0$; b, $L=3$; c, $L=5$; and d, $L=6$.

Surface steps are not expected to be perfect, and a realistic model must in some way account for the possible presence of vacancies, kinks, and other imperfections. Our approach allows us to consider readily the effects caused by kinks on the step edges. We take a kink to be the situation in which a portion of the step-edge atoms is shifted either forward or backward in the x direction by one lattice spacing. We can ignore the details of the amplitude scattered by the immediate vicinity of the kink, as this will be scattered mainly in directions away from the plane of incidence and the experiment only measures the in-plane intensity. The major effects on the in-plane intensity are the phase-shift interferences arising from the portions of the step edges at different lateral positions. These phase shifts are readily introduced into the structure factor (6) together with a weighting factor, depending on the density and number of kink positions. A typical calculation is shown in Fig. 4 for $\rho=0.05, L=12$ and each step having alternating forward and backward kinks and equal lengths of the step edge in each position. As might be expected, the kinks tend to wash out the structure far away from the diffraction peaks, while leaving the side bands nearest the diffraction positions relatively unaffected.

In general, the steps on a surface will be distributed over a number of different terrace levels. In order to obtain a model which predicts the intensity patterns observed experimentally, we have considered three different types of step distributions in the two dimensions parallel and perpendicular to the surface plane. Platinum has a fcc structure so the terrace atoms on different levels will have ABC stacking, and this feature must be included in any model for the Pt data. The three different step distributions are a random height model, a sawtooth distribution, and a random walk. All three of these models are constrained to a limited number of terrace levels lying between a maximum and a minimum height. The random walk has the steps either up or down in a constrained random walk within the finite number of levels. The sawtooth distribution has steps only in one direction (either up or down) until the maximum or minimum height is reached, after which the pattern is started again. This is a good representation of surface whose steps are the result of a slight miscut angle with respect to the symmetry plane, or surfaces in which the steps follow broad undulations of the height about the surface plane. The random height model chooses randomly both the direction of the step (up or down) and its height (within the constraint of maximum and minimum levels). We find that the results can be extremely sensitive to differences and nuances in the models, which implies that experiments of this type can be a powerful tool in distinguishing between different step distributions. The structure factors calculated with these two-dimensional models depend on all three components of the change in particle wave vector, as opposed to the one-dimensional models discussed above which depend only on the parallel wave-vector component. This means that the two-dimensional structure factors will depend on the choice of incident wave vector. Strong effects can occur depending on the phase or antiphase conditions for three-dimensional Bragg diffraction. This fact has recently been exploited in an extensive series of experiments and analyses by Hinch and Toennies.[29]

Figure 5 is an example of the sawtooth model and

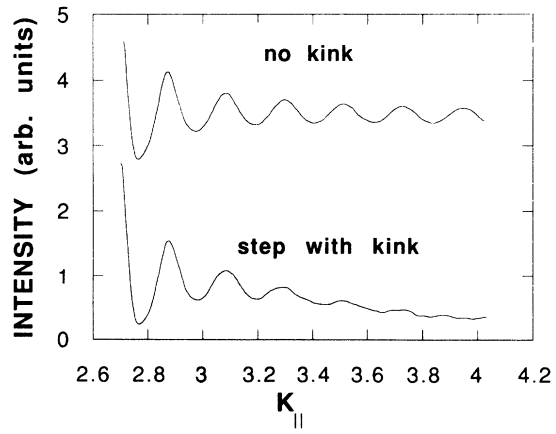

FIG. 4. The one-dimensional structure factor for a distribution with and without kinks. $\rho=0.05$ and $L=12$.

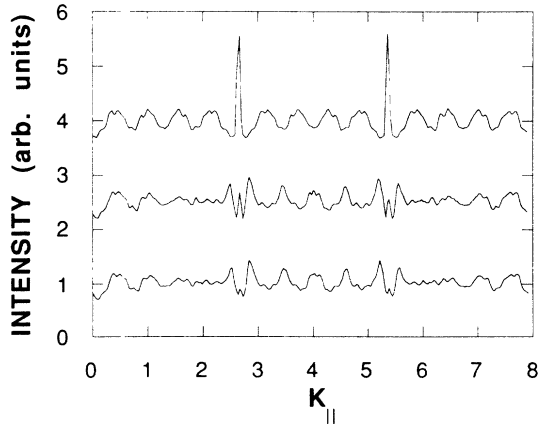

FIG. 5. Comparing ABC to AAA and ABA stacking for the sawtooth structure model. The number of terrace levels is 3, $L=4$, and $\rho=0.1$. Top curve is AAA, middle curve is ABA, and lower curve is ABC.

shows the importance of the threefold symmetry of the fcc surface. A surface with ABC stacking is compared with an AAA and an ABA surface. Note the strong central diffraction peak in the AAA structure factor which is weaker for the ABA and nearly absent in the ABC case.

The random height distribution is the least physical of the three that we have considered. The principal feature that is noted with this distribution is that as the number of levels is increased beyond two or three; the fine structure in the structure factor is rather quickly wiped out. This is especially true under incident beam and detector conditions in the neighborhood of antiphase conditions for three-dimensional Bragg diffraction.

The most relevant distribution to the Pt experiments is the random walk. This is because the steps were created by very low-energy ion bombardment on a smooth Pt(111) surface which originally had no measurable steps within the coherence length of greater than 1000 Å.[4] The average surface remains flat with probably only a few terrace levels. The random walk was the only one of the three models which could be made to agree with the available data. Figure 6 shows the structure factor for $\rho=0.075, L=4$ as a function of number n of terrace levels ranging between 2 and 6. All of the fine structure between diffraction peak positions decays away as n increases except for the sidebands. Very interestingly, the diffraction peak is also attenuated and completely disappears for $n>3$. This agrees nicely with the experimental observations shown in Fig. 7, where it is seen that in nearly all cases the fine structure appears as two split peaks about $\Delta K=G$, whenever G is near the apex of one of the broad oscillations, with no peak features precisely at the diffraction point G. The complete disappearance of the diffraction peak is a function of incidence conditions, and under in-phase Bragg conditions the central peak may remain strong.[29]

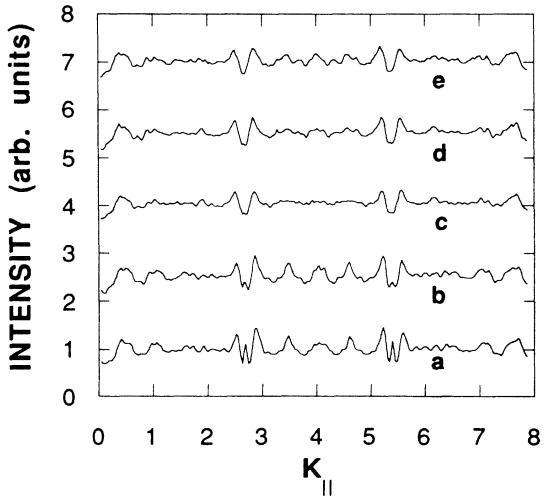

FIG. 6. Varying the number n of levels for the random walk distribution. $\rho=0.1$ and $L=4$. a, $n=2$; b, $n=3$; c, $n=4$; d, $n=5$; and e, $n=6$.

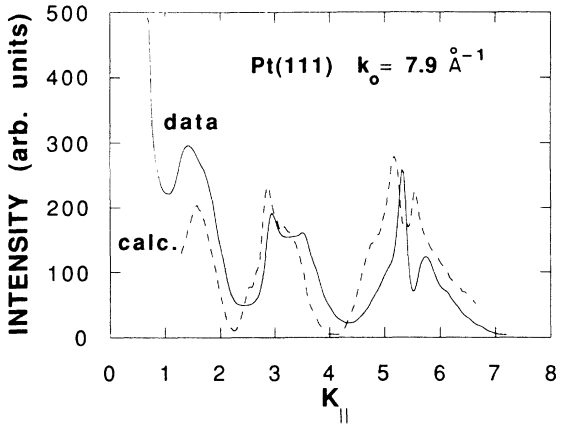

FIG. 7. Comparison of calculations with data for He scattering from a Pt(111) surface contaminated with steps. The dashed lines are calculations and the solid curves are data. The wave vector is 7.9 Å^{-1}.

Figures 7 and 8 show the best fit to the experimental data for the two incident conditions using the random walk model. For each incident energy the structure factor has been multiplied by the appropriate form factor calculated in Sec. IV and shown in Figs. 1 and 2. The other parameters are $\rho=0.1$ and $L=4$, and it was deemed essential to take ABC stacking into account. This model, without change of parameters, successfully fits the data taken at the two different choices of incident energy.

VI. CONCLUSIONS

From this work we can draw the conclusion that the primary cause of the fine structure in the experimental data for He backscattered from a dilute distribution of steps on a surface is the ordering arising from the step positions on lattice sites. The problem of atom scattering from a dilute distribution of noninteracting steps on a flat surface can be characterized by the product of a form factor giving the reflected intensity of a single step multi-

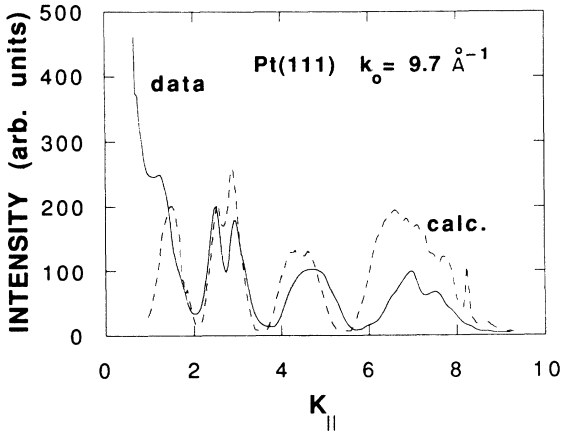

FIG. 8. Same as Fig. 7 except for a wave vector of 9.7 Å^{-1}.

plied by a structure factor for the distribution of steps. For the form factor, we have developed a Green-function method applied to a hard-core profile. Calculations in the eikonal limit, taking into consideration the attractive adsorption well in front of the step, describe well the broad oscillations characteristic of single-step scatering intensities. The structure factor is calculated using a number of lattice-gas models, incorporating the repulsive force between adjacent steps through an imposed minimum distance between nearest neighbors. Numerous calculations have been carried out[30] which show that the structure factor is quite sensitive to the statistics of the step distribution, to the density of steps, and to the number of terrace levels over which they are distributed. The presence of kinks along the step edges is shown to rapidly attenuate fine details in the structure factor, especially for wave-vector values in between diffraction peak positions.

We examine the data for scattering of He from Pt(111) surfaces contaminated with steps, and find good agreement between our models and the measured intensities. The splitting of the fine structure around diffraction peak positions indicates the nearest-neighbor distance between steps, and it is necessary to take into account the *ABC* stacking symmetry of the (111) surface. The results also indicate the density of steps and the number of terrace levels over which they are distributed.

All surfaces, no matter how well prepared, seem to include a small but irreducible number of defects,[31] and one of the most common defects is steps. Steps can occur on ordered surfaces,[19] as a result of intentional disordering,[4,32] or in the process of crystal growth.[33,34] The strong sensitivity of the diffuse elastic reflected intensity to the details of the step distribution shows that measurements of this type should be extremely useful in characterizing the structure of such surface defects.

ACKNOWLEDGMENTS

We would like to thank B. J. Hinch and J. P. Toennies for helpful discussions.

*Present address: Naval Research Laboratory (Code 6341), Washington, D.C. 20375-5000.

[1]T. Engel and K. H. Rieder, *Structural Studies of Surfaces* (Springer-Verlag, Berlin, 1982); J. P. Toennies, Appl. Phys. **3**, 91 (1982).
[2]B. Poelsema, L. K. Verheij, and G. Comsa, Phys. Rev. Lett. **49**, 1931 (1982).
[3]B. Poelsema, G. Mechtersheimer, and G. Comsa, Surf. Sci. **111**, 519 (1981).
[4]A. M. Lahee, J. R. Manson, J. P. Toennies, and Ch. Wöll, Phys. Rev. Lett. **57**, 471 (1986).
[5]A. M. Lahee, J. R. Manson, J. P. Toennies, and Ch. Wöll, J. Chem. Phys. (to be published).
[6]G. Drolshagen and R. Vollmer, J. Chem. Phys. **87**, 4948 (1987).
[7]B. J. Hinch, Phys. Rev. B **38**, 5260 (1988).
[8]J. R. Manson and V. Celli, Phys. Rev. B **39**, 3605 (1989).
[9]L. Van Hove, Phys. Rev. **95**, 249 (1954).
[10]G. Drolshagen and E. Heller, J. Chem. Phys. **79**, 2072 (1983).
[11]B. J. Hinch, A. Lock, J. P. Toennies, and G. Zhang, J. Vac. Sci. Technol. (to be published).
[12]U. Garibaldi, A. C. Levi, R. Spadacini, and G. E. Tommei, Surf. Sci. **48**, 649 (1975).
[13]B. J. Hinch, Surf. Sci. (to be published).
[14]H. Jonsson, J. H. Weare, and A. C. Levi, Phys. Rev. B **30**, 2241 (1984).
[15]P. M. Morse and H. Feshbach, *Methods of Theoretical Physics* (McGraw-Hill, New York, 1953), Chap. 11.
[16]V. Celli, in *Many-Body Phenomena at Surfaces*, edited by D. Langreth and H. Suhl (Academic, New York, 1984), p. 315.
[17]A. M. Lahee, R. J. Blake, and W. Allison, Surf. Sci. **151**, L153 (1985).
[18]J. L. Beeby, J. Phys. C **5**, 3438 (1972); **5**, 3457 (1972).
[19]J. Perreau and J. Lapujoulade, Surf. Sci. **119**, L292 (1982); **122**, 341 (1982).
[20]A. T. Yinnon, R. Kosloff, and R. B. Gerber, J. Chem. Phys. **88**, 1 (1988).
[21]M. Henzler, in *Electron Spectroscopy for Surface Analysis*, edited by H. Ibach (Springer-Verlag, Heidelberg, 1977), p. 177.
[22]G. Comsa, Surf. Sci. **81**, 57 (1979).
[23]T. M. Lu and M. G. Lagally, Surf. Sci. **99**, 695 (1980).
[24]D. R. Frankl, Surf. Sci. **91**, 365 (1980).
[25]G. C. Wang and M. G. Lagally, Surf. Sci. **81**, 69 (1979).
[26]J. E. Houston and R. L. Park, Surf. Sci. **21**, 209 (1970).
[27]J. E. Houston and R. L. Park, Surf. Sci. **26**, 269 (1971).
[28]C. S. Lent and P. I. Cohen, Surf. Sci. **139**, 121 (1984).
[29]B. J. Hinch and J. P. Toennies (unpublished).
[30]C. W. Skorupka, Ph.D. thesis, Clemson University, 1989.
[31]G. Armand, J. Lapujoulade, and J. R. Manson, Phys. Rev. B **39**, 10 514 (1989).
[32]B. Poelsema, L. K. Verheij, and G. Comsa, Phys. Rev. Lett. **53**, 2500 (1984).
[33]L. J. Gomez, S. Bourgeal, J. Ibanez, and M. Salmeron, Phys. Rev. B **31**, 2551 (1985).
[34]B. J. Hinch, C. Koziol, J. P. Toennies, and G. Zhang (unpublished).